

The characteristics of studying high speed motorized spindle dynamic magnetic coupled

Z Ke¹, W Zinan^{1*} and W Qingyuan¹

¹ School of Mechanical Engineering, Shenyang Jianzhu University, National and Local Joint Engineering Laboratory of High-grade Stone Numerical Control Processing Equipment and Technology, Hunnan East Road on the 9th, Hunnan District, Shenyang, China. Postcard: 110168

*E-mail: wzn591672678@126.com

Abstract: The vibration of high speed motorized spindle directly influences the processing quality; through the finite element method, the dynamic magnetic coupling model of high speed motorized spindle rotor system is established. The coupling relationship between the field parameters of electromagnetic and the characteristics of dynamic are considered. At the same time, the influence of electromagnetic coupled on the dynamic vibration characteristics of the rotor system is analysed and the experimental verification is carried out. The results indicate the stator and rotor magnetic density, the magnetic field energy distribution about motorized spindle are also periodic. The skin effect of magnetic field and air gap eccentricity have great influence on radial vibration. With the increase of speed, the centrifugal force of the bearing is increasing; the softening effect of bearing stiffness is obvious; the natural frequency is decreasing; the amplitude of vibration is increasing. The experimental results are in good agreement with the simulation results. The accuracy of the dynamic magnetic coupling model is illustrated.

1. Introduction

The motorized spindle basic characteristics of high speed, high rotation accuracy and small vibration are the important factors to ensure the reliability of machine tools. Scholars at home and abroad have done a lot of motorized spindle research on the electric field, magnetic field and dynamics. Masoud Razban and Mohammad R. Movahhedy [1] considered the gyroscopic effect, an automatic variable pressure preload system was put forward. Atsushi Matsubara [2], through non-contact excitation, evaluated the method of dynamic stiffness on the motorized spindle. O. Öz, Ahina [3] predicted the dynamic performance of motorized spindle and bearing through the FRF response function. CaoHongrui [4] put forward the six concepts of motorized spindle balance, motorized spindle health and so on. Chen Xiaolan [5] analysed the vibration shape of rotor rigid body and proposed the theory of active inhibition. Zhang Ke [6, 7] designed a vector controller based on slip frequency control. The coupling relationship between the thermal characteristics and the vibration characteristics of the motorized spindle is obtained. Fourier transform, polynomial curve fitting and Hooke's law are combined to design and develop an algorithm for measuring the magnitude of dynamic imbalance force, vector position and direction of motorized spindle. Zhang Lixiu [8, 9] established that the a multi-field coupling model is to predict the dynamic performance of motorized spindle, and the



control performance of motorized spindle is improved by using ANN and CBR. Wang Bo [10] completed the finite element modelling of motorized spindle system based on the modelling idea of the parallel rotor. All the above studies aim at single dynamic analysis. The influence of electromagnetic force and electromagnetic torque on motorized spindle dynamics are neglected. Especially, the electromagnetic model is not integrated into the dynamic model, which is not a comprehensive consideration of the dynamic characteristics.

In view of the above shortcomings, a new dynamic magnetic coupled model is established in this paper. The coupling relationship between motorized spindle system dynamics and electromagnetism is analyzed. The influence of different electromagnetic force and torque on dynamics is discussed. At the same time, the unbalanced magnetic pull and the centrifugal force of the bearing are used to establish the dynamic model, which is closer to the actual working condition. Finally, the test verifies the accuracy of the model.

2. The establishment of dynamic magnetic coupled model

2.1. The structure diagram of dynamic magnetic coupled model

Due to the change of air gap between the rotor and stator, electromagnetic parameters, such as current, magnetic field, magnetic flux and so on are motivating magnetic force and torque influencing the dynamics of motorized spindle. Figure 1 is the structure diagram of high speed motorized spindle dynamic magnetic coupled.

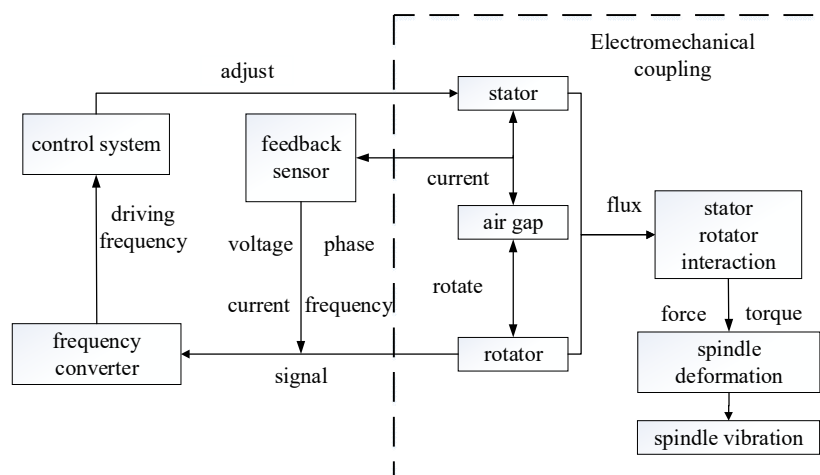


Figure 1. The structure diagram of high speed motorized spindle dynamic magnetic coupled.

The air gap of motorized spindle is the gap of between stator fixed and rotor rotated pole. On the one hand, the air gap affects the dynamic performance of motorized spindle, the unbalanced magnetic pull produced by eccentric operation as a non-negligible external load is the important factor of motorized spindle vibration. On the other hand, the magnetic flux leakage and loss generated by air gap determine the electromagnetic parameters. Electromagnetic force, torque and other electromagnetic factors are the basic conditions of the velocity and other parameters in dynamics.

2.2. The establishment of dynamic magnetic coupled model for motorized spindle

2.2.1. The establishment of electromagnetic model. The main components of the high-speed motorized spindle, the shell, stator and rotor are simplified as cylinders, and the magnetic field model of the motorized spindle is established.

The Bessel function is applied to make the motorized spindle rotor equivalent to the magnetic field of the cylinder [11]. Using the m order imaginary Bessel equation, we can obtain:

$$x^2 \frac{d^2 R}{dx^2} + x \frac{dR}{dx} + (x^2 - m^2)R = 0 \quad (1)$$

$$x = \sqrt{\mu\rho} \quad (2)$$

Because the motorized spindle is a symmetrical circular annular current, the vector potential A of the air gap is solved.

$$A = \frac{\mu}{4\pi} \int_V \frac{J'(r') dV'}{R} \quad (3)$$

$$J(r') = e_\varphi J_\varphi(\rho', z') \quad (4)$$

There are different magnetization effects between the air gap of the motorized spindle. The medium is magnetized, generating the intensity of the magnetic field, which is:

$$B = \mu_0(1 + \chi_m)H = \mu_0\mu_r H \quad (5)$$

μ_0 —Vacuum magnetic permeability, χ_m —medium magnetic susceptibility, μ_r —relative magnetic permeability, H—medium magnetic field intensity vector

The motorized spindle rotate speed of rotor:

$$v = 2p\tau \frac{n_1}{60} = 2\tau f_1 \quad (6)$$

l —the effective length of stator and rotor, v —the velocity of the rotating magnetic field in the air gap, τ —the center point distance of adjacent magnetic poles in rotating magnetic field

According to the dynamic equation, motorized spindle induction strength and electromotive force, the radial force of XY axis about rotor system is obtained.

$$\begin{bmatrix} F_{1x} \\ F_{1y} \end{bmatrix}_{i+1,j+1} = \begin{bmatrix} f_{1x} \\ f_{1y} \end{bmatrix}_{i,j} \begin{bmatrix} D_{ii} & D_{ij} \\ D_{ji} & D_{jj} \end{bmatrix} \begin{bmatrix} S_i \\ S_j \end{bmatrix} \quad (7)$$

Unbalanced magnetic pull and radial force in rotor system

$$\begin{cases} f_e = k_{xx}x + k_{xy}y + c_{xx}\dot{x} + c_{xy}\dot{y} \\ f_r = k_{yx}x + k_{yy}y + c_{yx}\dot{x} + c_{yy}\dot{y} \end{cases} \quad (8)$$

ε_{ij} —The eccentricity of air gap, S—contact surface area of stator and rotor

2.2.2. The establishment of loss model. According to the input parameters of frequency converter, the motorized spindle input power is known.

$$P_1 = 3U_0 I_0 \cos \varphi_1 \quad (9)$$

$\cos \varphi_1$ —the power factor of motorized spindle, U_0 、 I_0 —the effective value of phase current and voltage, φ_1 —the angle between phase voltage and phase current

The stator and rotor are made of copper wire winding, copper loss is

$$P_{cu} = 3(I_1^2 + I_2^2)R_2 \quad (10)$$

Mechanical power is:

$$P_m = P_1 - P_{cu} \quad (11)$$

Electromagnetic torque is:

$$T_{em} = \frac{P_m}{\Omega} = \frac{30pP_m}{\omega\pi n_1} \quad (12)$$

P —pole of the rotor Ω —the angular velocity of synchronous mechanical

2.2.3. Dynamics equation. Calculation of dynamic characteristics of motorized spindle based on the Timoshenko beam element theory [12]. The dynamic balance equation of the motorized spindle structure is established.

$$M\ddot{x}(t) + (C + G)\dot{x}(t) + Kx(t) = T_{em} + F_e + F_r \quad (13)$$

M —Mass matrix of motorized spindle, C —Damping matrix of motorized spindle

G —Gyroscopic effect matrix of bearing, K —Support stiffness matrix of motorized spindle

T_{em} —Electromagnetic torque of motorized spindle, F_e —Unbalanced magnetic pull

F_r —Electromagnetic radial force

Natural frequency of motorized spindle

$$\omega = \sqrt{\frac{K}{M}} \quad (14)$$

Rayleigh damping

$$C = a_0 K + a_1 M \quad (15)$$

$$\begin{pmatrix} a_0 \\ a_1 \end{pmatrix} = 2 \frac{\omega_m \omega_n}{\omega_n^2 - \omega_m^2} \begin{pmatrix} \omega_n & -\omega_m \\ -1/\omega_n & 1/\omega_m \end{pmatrix} \begin{pmatrix} \xi_m \\ \xi_n \end{pmatrix} \quad (16)$$

ξ_m and ξ_n are the different frequencies of the motorized spindle material ω_m, ω_n , Respectively the corresponding damping ratio are 0.05 and 0.08. ω , which is the natural frequency of a motorized spindle.

3. The analysis of electromagnetic field

The magnetic field model of the motorized spindle is established through the finite element ANSYS software electromagnetic module, and the magnetic density of the stator and rotor, electromagnetic energy distribution diagram and torque diagram are calculated. The establishment of a fixed rotor model is assumed as follows, ignoring the external magnetic field interference and axial variation of the magnetic field. Only considering the variation of the radial magnetic field, a two dimensional model is selected.

3.1. The establishment of rotor model for motorized spindle

Parameter setting of electric motorized spindle: pole of the rotor is 2, number of stator slots is $Z_1=24$, number of rotor slots is $Z_2=28$, external diameter of stator is 130mm, internal diameter of stator is 80mm, air gap is 0.3mm, external diameter of rotor is 79.4 mm, internal diameter of rotor is 51mm.

According to the electromagnetic model of the motorized spindle, the rotor is uniformly rotated in the stator, so the time stepping method is used to calculate the two time's stator and rotor magnetic dense cloud diagram, as is shown in figure 2. It can be seen that figure 2 shows a circumferential symmetry distribution of magnetic flux density. The interior of the stator and the outside of the rotor are densely distributed. The magnetic density is mainly concentrated in the magnetic pole and the surrounding area. The interior of the rotor and the outside of the stator are less affected by air gap. The magnetic density distribution is uniform and more and more scarce. Because of the high speed frequency conversion of the motorized spindle, the eddy current of the magnetic field generated by cutting the magnetic line, which results in the skin effect leading the maximum magnetic density of the contact magnetic pole on rotor and stator. Firstly, it is in the state of saturation, the magnetic flux is limited by air gap magnetic density. The magnetic lines of force are bending. The magnetic flux enters the inner

edge region of the rotor to form a magnetic circuit closure. The internal magnetic density of the rotor is the least. The magnetic flux is permeable to the adjacent magnetic pole. The magnetic flux density of the adjacent poles increases and the reduced phenomenon of magnetic appears in the radial direction of the stator and rotor.

As compared to figure 2(a) and (b), it is known that the transfer rate becomes larger. The distribution of the magnetic pole density of the fixed rotor is gradually reduced. The magnetic flux density line diffuses along the outer side of the stator and the inner part of the rotor. The magnetic flux eddy current phenomenon is more obvious. The close magnetic density periphery of the magnetic stator and rotor pole is increased. The density of the adjacent magnetic poles of the adjacent magnetic poles is reduced.

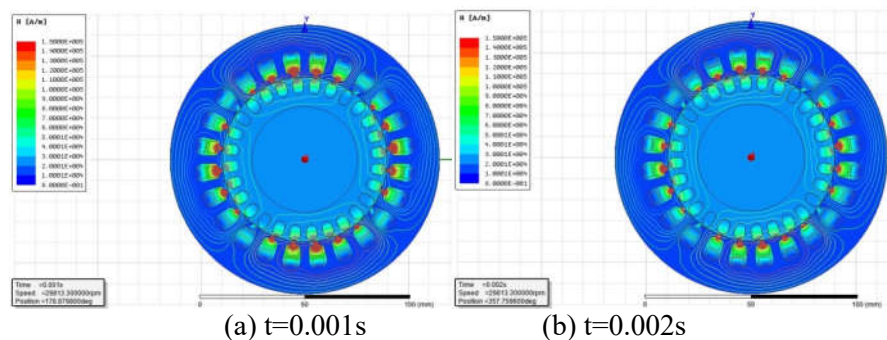


Figure 2. The cloud diagram of stator and rotor magnetic flux density.

3.2. Calculation and analysis of electromagnetic field performance of motorized spindle

According to the electromagnetic model of motorized spindle, the energy diagram of motorized spindle which is obtained, as is shown in figure 3. At the beginning of 0.001-0.003s, the peak value of the electric field and the magnetic field energy appears. The peak value of electromagnetic energy coincides with the maximum value of electromagnetic energy in figure 3. The accuracy of the electromagnetic model of the electric motorized spindle is reflected. The electric field energy decreases rapidly in time. After running smoothly, the electric field tends to be stable and no longer attenuates. The regularity fluctuate is periodicity. The energy of the magnetic field starts to increase rapidly. Rapid magnetic circuit saturation occurs between the magnetic poles of stator and rotor. The magnetic flux diffusion is limited. After the smooth operation, the magnetic circuit slows down.

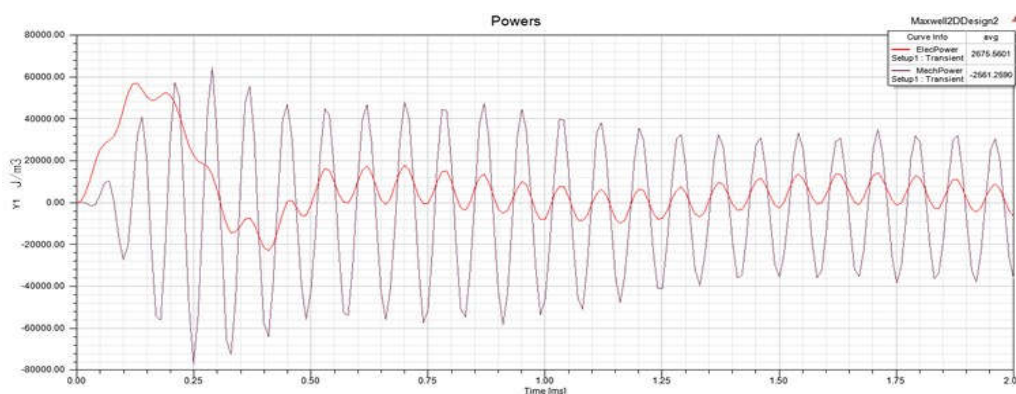


Figure 3. The energy curve of motorized spindle.

The main reason that affects the magnetic density is the difference between the poles of the stator poles and the uneven magnetic poles of the air gap. The uneven air gap poles the main reason for the radial force. Combined with figure 2, due to the distribution of the symmetrical magnetic density, analysing a periodic region of magnetic density distribution is needed.

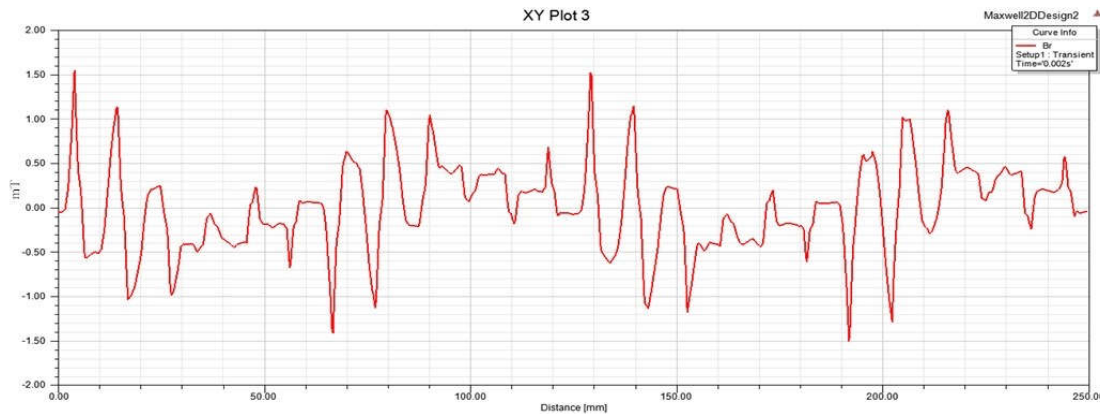


Figure 4. The radial magnetic density diagram of motorized spindle.

4. Dynamic performance analysis of motorized spindle

The exciting force of motorized spindle is mainly composed of random excitation force and steady state exciting force. The steady state exciting force mainly consists of electromagnetic torque, radial force, bearing centrifugal force and preload force, etc. The steady state exciting force of motorized spindle is loaded into the dynamic model of motorized spindle. The influence of multiple factors on motorized spindle vibration and bearing stiffness and frequency is calculated by means of the Kriging algorithm.

$$\bar{y}(x) = \sum_{i=1}^k \beta_i f_i(x) + Z(x) = f^T(x)\beta + Z(x) \quad (17)$$

$f^T(x)$ is base function vector of radial force regression motorized spindle model, β is the centrifugal force, gyroscopic moment and other parameters of the regression motorized spindle model. The approximate equivalent of electromagnetic torque is the normal distribution function. $N(0, \sigma^2)$ is a random function that obeys the normal distribution, the function covariance is:

$$\text{cov}(Z(x_1), Z(x_2)) = \sigma^2 R(x_1, x_2) \quad (18)$$

$R(x_1, x_2)$ is the correlation equation between x_1 and x_2 two electromagnetic data points. Gauss function is applied to find the dependencies between variogram and covariance function to guarantee the smoothness of the semi variant function.

The Monte Carlo method is used to generate motorized spindle dynamic data samples

$$y(x) = \beta + r^T(x)R^{-1}(Y - f\beta) \quad (19)$$

$y(x)$ is the vibration fitting curve of the electric motorized spindle.

The B7009C/P4 bearing of the front bearing of the ceramic motorized spindle is taken as an example. The parameters of the front bearing are shown in table 1. The front bearing is preloaded with constant pressure. The bearing preload force is 600N. The process of the experiment is that the motorized spindle speed is 0-18000rpm.

Table 1. The parameters of front bearing.

Bearing type	Ball material	d_m (mm)	D_b (mm)	N	$A(^{\circ})$	v
B7009C/P4	Si_3N_4	60	7.5	19	15	0.3

The air gap eccentricity of the motorized spindle is affected by the centrifugal force, the gyroscopic moment of the bearing and assembly. The air gap magnetic field energy and electromagnetic torque of the motorized spindle are changed. The simulation results show that the normal and eccentric vibration

spectrum under no-load operation condition of the motorized spindle is shown in figure 5. The trend of vibration track for normal and eccentric operation is basically the same. But the vibration amplitude of eccentric operation is much larger than that of normal operation. The results show that the air gap eccentricity causes the torque of the fixed rotor, the magnetic field distribution is not uniform, the torque and radial force amplitude is much larger than the normal running condition. The unbalanced magnetic pull causes the radial vibration of motorized spindle shell to increase.

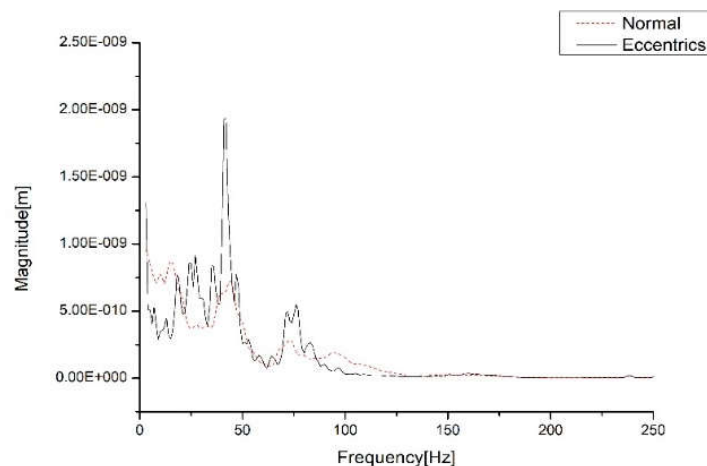


Figure 5. Normal and eccentric vibration spectrum of motorized spindle.

In the motorized spindle high-speed test, the natural frequency of the motorized spindle is mainly affected by the centrifugal force of the bearing. The stiffness of the bearing is changing as the speed changes. With the increase of the rotating shaft, the centrifugal force of the bearing increases the contact deformation of the angular contact ball bearing outer ring and outer ring groove. The contact between inner ring and inner race decreases, and the stiffness of radial support is softened. The stiffness softening causes the reduction of the natural frequency of the motorized spindle. At the speed of 6000rpm, the experimental data were measured by hammering. From figure 6, it can be seen that the experiment is in general in agreement with the simulation data. The first natural frequency of simulation is 1125HZ, and the data obtained from the experiment is 1110HZ, the difference between them is 15HZ. It can be seen that the bearing stiffness is softened and, together with the gyroscopic effect, it is the important factor that causes the natural frequency of the test to be lower than the natural frequency of simulation. It can be seen from the diagram that the simulation results agree well with the experimental values, indicating the accuracy of the motorized spindle bearing system model.

Three experiments have been taken to verify the reliability of the electromagnetic coupling simulation system of the motorized spindle. The rotational speed is designed for 6000rpm, 12000rpm, and 18000rpm to collect the displacement sensor signals to form the vibration displacement diagram of the motorized spindle. In figure 7 (a), it can be seen that the motorized spindle speed is the direct factor determining the amplitude of vibration. Due to the fact that the centrifugal force acts on the bearing inner ring, the inner ring displays expansion and deformation. The inner ring expansion is greater than the rotor expansion, and the interference amount of the bearing inner ring and the rotor is reduced. The radial stiffness of the bearing decreases with the increase of the speed, and the radial vibration of the bearing becomes larger. The contrast in figures 7 (a) and (b) show that, despite the simulation and experiment in motorized spindle 18000rpm, the maximum amplitude value difference is a 10^{-8} m error. There are many electromagnetic interfering factors, such as external magnetic field, magnetic leakage and so on. The trend of simulation and experimental model can be consistent. The reliability of dynamic magnetic coupling model of high-speed motorized spindle is verified.

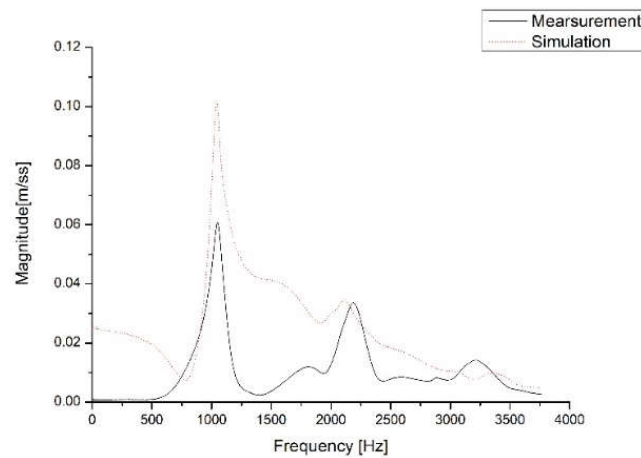
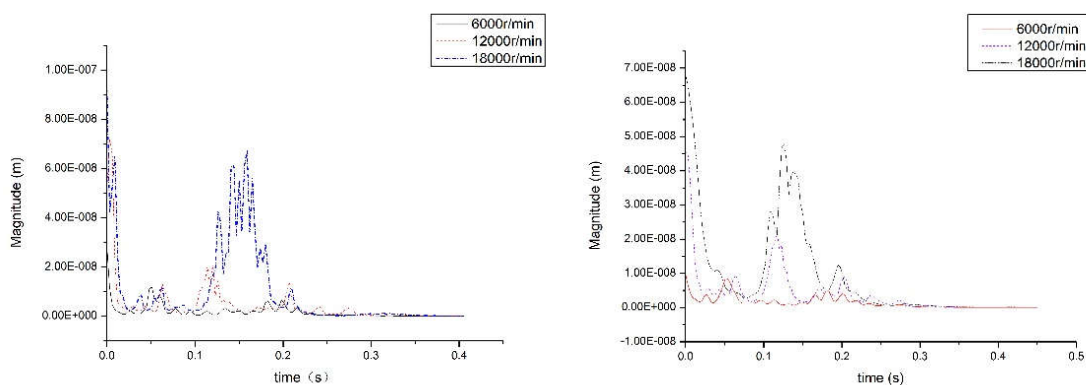


Figure 6. The diagram of natural frequency response function.



(a) The diagram of test vibration displacement (b) The diagram of simulate vibration displacement

Figure 7. The vibration displacement diagram of motorized spindle.

5. Conclusion

(1) The magnetic flux density and electromagnetic energy of high-speed motorized spindle stator and rotor are periodic distribution with time. The influence of the skin effect of the magnetic field and air gap eccentricity on the distribution of magnetic field is obvious. Unbalanced magnetic tension formed by gas gap eccentricity has a direct connection with the radial vibration of the motorized spindle.

(2) During the high-speed operation of the rotor and the inner ring of the motorized spindle, the centrifugal force makes the contact deformation of the angular contact ball bearing outer ring and outer ring groove increase. The contact between inner ring and inner race decreases, the inner ring of the bearing expansion is deformed, and the expansion of the inner ring is larger than that of the rotor. The interference between bearing inner ring and rotor decreases, the radial stiffness of bearing decreases with the increase of the rotational speed, and the radial vibration becomes larger.

(3) The electromagnetic field and other parameters are coupled into the dynamic model. The coupling relationship between the dynamic and the magnetic model has been analysed. The influence of multi factors coupling on dynamic vibration characteristics has been studied. The error between simulation results and experimental results is small, which reflects the accuracy of the dynamic magnetic coupling model.

Acknowledgments

The article is supported by Shenyang science and technology program project F16-096-1-00, National Natural Science Fund 51675353 and The innovation team project about the Ministry of Education IRT-15R45.

References

- [1] Razban M and Movahhedy M R 2015 A speed-dependent variable preload system for high speed spindle *Prec. Eng.* **40** 182
- [2] Matsubara A, Tsujimoto S and Kono D 2015 Evaluation of dynamic stiffness of machine tool spindle by non-contact excitation tests *CIRP Annals-Manuf. Tech.* **64** 365
- [3] Özsahina O, Budakb E and Özgüven H N 2015 Identification of bearing dynamics under operational conditions for chatter stability prediction in high speed machining operations *Prec. Eng.* **42** 53
- [4] Cao H, Zhang X and Chenba X 2017 The concept and progress of intelligent spindles: A review *Int. J. of Machine Tools & Manuf.* **112** 21
- [5] Xiaoan C, Peng Z, Ye H and Jun-feng L 2014 Axial vibration of high-speed motorized spindles *J. of vibration and shock* **33** (20) 70
- [6] Ke Z, Tong L, Huabo D and Yuhou W 2016 A Motorized Spindle Online Dynamic Balance Testing Algorithm *J. of Shenyang Jianzhu Univ. (Natural Science)* **32** (1) 148
- [7] Ke Z, Zhixue L, Lixiu Z, Ying X and Yuhou W 2012 Modeling of High- Speed Motorized Spindle and Design and Simulation Research of Vector Controller Based on Slip Frequency Control *J. of Shenyang Jianzhu Univ. (Natural Science)* **28** (6) 1114
- [8] Lixiu Z, Yuhou W and Jinxiang P 2013 The Method about Stator Resistance Hybrid Intelligent Identification of Motorized Spindle *J. of Shenyang Jianzhu Univ. (Natural Science)* **29** (6) 1099
- [9] Lixiu Z, Ming Y, Yuhou W and Feng L 2016 Multi-field coupled model and dynamic performance prediction for 150MD24Z7.5 motorized spindle *J. of vibr. and shock* **35** (1) 59
- [10] Bo W, Wei S and Bangchun W 2012 The Finite Element Modeling of High-speed Spindle System Dynamics with Spindle-holder-tool Joints *J. of Mech.Eng.* **48** (15) 83
- [11] Zhongkui Z and Lixia C 2012 The Application of Bessel Function in Solving Variable Coefficient Differential Equation *J. of Jiamusi Univ. (Natural Science Edition)* **30** (6) 926
- [12] Xiaofeng W and Qing-shan Y 2008 Coupled bend and torsion analysis of the spatial thin-walled beam using timoshenko theory *Eng. Mech.* **25** (5) 12